Exceptionally Preserved Conodont Natural Assemblages from the Middle Triassic Luoping Biota, Yunnan Province, China: Implications for Architecture of Conodont Feeding Apparatus

Jinyuan Huang [*1, 2, 3], **Carlos Martínez-Pérez**[2], **Qiyue Zhang**[1], **Kexin Zhang**[3], **Mao Luo**[4],
Wen Wen[1, 5], **Changyong Zhou**[1], **Xiao Min**[1], **Zhixin Ma**[1, 6], **Tao Xie**[1], **Michael J. Benton**[7],
Philip C. J. Donoghue[7]

1. *Chengdu Center, China Geological Survey (Geosciences Innovation Center of Southwest China), Chengdu 610081, China*
2. *Cavanilles Institute of Biodiversity & Evolutionary Biology, University of Valencia, 46980 Valencia, Spain*
3. *Institute of Geological Survey, China University of Geosciences, Wuhan 430074, China*
4. *State Key Laboratory of Palaeobiology and Stratigraphy, Nanjing Institute of Geology and Palaeontology and Center for Excellence in Life and Paleoenvironment, Chinese Academy of Sciences, Nanjing 210008, China*
5. *School of Earth Sciences and Engineering, Nanjing University, Nanjing 210023, China*
6. *School of Ocean Sciences, China University of Geosciences, Beijing 100083, China*
7. *School of Earth Sciences, University of Bristol, Bristol BS8 1TQ, UK*

Jinyuan Huang: https://orcid.org/0000-0002-3739-3114

ABSTRACT: Articulated natural assemblages contain direct evidence of the element numbers, morphologies, positions and structures for reconstructing the feeding apparatuses of conodont animals, but these kind of materials are very rare in fossil records. Here we report ten new conodont natural assemblages from Member II of the Guanling Formation in Luoping County, eastern Yunnan Province, southwestern China. These assemblages were obtained from the fossil-bearing layers of the Luoping Biota, dated to the early Middle Triassic Anisian stage (Pelsonian substage). These fossiliferous laminated limestones mainly consist of calcites and dolomites, with platy clay minerals and pyrites as subordinate components, indicating that the conodont assemblages were preserved in a lower energy and anoxic sedimentary environment. The new natural assemblages preserve the primary collapse orientations of the *Nicoraella* feeding apparatus from the Luoping Biota, showing the relative original positions of the S, M and P elements, that could be further used to refine the architecture of this apparatus in space variable M elements and the position unclear P_1 elements. Integrating previously reported three-dimensional and bilaterally symmetrical fused clusters, we statistically analyze the size of the positional homogenous elements within different sized materials, in particular S_4, S_3, or S_2 elements, indicates that elements ontogenic changes do not affect the apparatus architecture. Architecture of *Nicoraella* apparatus remains stable in the process of ontogeny, so our reconstructed model is credible. It is the first time that ample types of materials have been used to restore a conodont apparatus within one genus, namely natural assemblages (articulated and disarticulated), fused clusters (articulated, disarticulated, compressed, and relatively three-dimensional), and abundant discrete elements, respectively. These materials together record the most complete information on architecture in the gondolelloid apparatuses, thus enabling us to reconstruct a reliable fifteen-element apparatus and propose it as a standard template for gondolelloid apparatus reconstruction.
KEY WORDS: conodont, natural assemblage, architecture, fused cluster, size variation, limestone, Middle Triassic, southwestern China.

0 INTRODUCTION

Conodont animals belong to an extinct group of primitive vertebrates (Janvier, 1995; Purnell et al., 1995; Aldridge et al., 1994), eel-shaped bodies, mainly comprised of soft tissues, except for a series of hard skeletal elements in the mouth part (Aldridge et al., 1993; Briggs et al., 1983; Higgins, 1983). The hard elements are regarded to perform 'feeding' functions (Purnell and Donoghue, 1997; Briggs et al., 1983). These regu-

larly arranged hard skeletal elements form the conodont feeding apparatus, occasionally preserved as clusters and natural assemblages on bedding surfaces, are crucial in understanding the apparatus structure, architecture, functional morphology, and evolutionary relationships in conodont animals (Goudemand et al., 2011; Donoghue et al., 2008; Purnell and Donoghue, 1997). Since the discovery of natural assemblages (Schmidt, 1934; Scott, 1934) and soft bodied conodont animals (von Bitter et al., 2007; Aldridge and Theron, 1993; Aldridge et al., 1993; Briggs and Clarkson, 1987; Briggs et al., 1983; Higgins, 1983), there has been a shift in conodont systematics from form taxonomy to multielement taxonomy (Sweet and Donoghue, 2001; Sweet and Bergström, 1969). More attention has been paid on the whole apparatus rather than single conodont element in order to understand the biology of conodonts.

Nowadays, the reconstruction of a reliable apparatus is the most important task to further understand apparatus function of conodonts. Previously, many apparatuses have been described in detail to interpret through the discrete elements (Wardlaw and Nestell, 2010; Mellgren and Eriksson, 2006; Zhang, 1998; etc.), or the components of clusters and natural assemblages (Huang et al., 2019a, b, c; Suttner et al., 2018; Zhang et al., 2017; Aldridge et al., 2013; Goudemand et al., 2012; Sun et al., 2009; Purnell and Donoghue, 1998, 1997; etc.). In particular, some fused clusters have been found to preserve exceptional three-dimensional structures, e. g., the *Nicoraella* clusters from the Luoping Biota, Yunnan Province, southwestern China (Huang et al., 2019b). Previous studies demonstrated several essential attributes of the ozarkodinin apparatus: (1) two series components of the apparatus flanked dextrally and sinistrally at conodont animals' mouth; (2) elements of the S-M and P arrays in bilaterally mirrored symmetry; (3) S-M arrays located rostrally, P elements settled caudally; (4) M elements placed outside the S array; and (5) morphological similarities of the corresponding locations in different genera of apparatuses. However, establishing a reliable architecture of the apparatus is difficult because most of assemblages and clusters are incomplete or highly compressed. Therefore, multi-aspect work on apparatus reconstruction is needed, and will allow us to better understand apparatus function and the feeding process of conodonts.

A great number of Triassic conodont apparatuses have been reconstructed formerly from Chinese materials. During 2011 and 2012, many fused clusters (Early Triassic) were obtained from several sites in Guangxi, South China. Among these, one cluster partially preserves the original arrangement of the S ramiform elements, and has been used to reconstruct an apparatus of *Novispathodus*. The results showed a new arrangement of the elements and suggested that conodonts were basal vertebrates based on the assumed pulley-shaped lingual cartilage (Goudemand et al., 2011). However, the architecture of the apparatus and the hypothetical cartilage were still uncertain, as the reconstruction was based upon incomplete fused clusters. More recently, several late Smithian conodont natural assemblages were discovered from East China (Sun et al., 2021, 2020). One came from the uppermost Lower Qinglong Formation at Longtan Section, Nanjing City, Jiangsu Province, and others from the uppermost Helongshan Formation of the South Majiashan Section, Chaohu City, Anhui Province. Two new ap-

paratuses (*Scythogondolella milleri* and *Hadrodontina aequabilis*) were reconstructed using synchrotron X-ray microtomography. Both contain 15 elements, but with different element morphologies: the apparatus of *Scythogondolella milleri* has eight types of elements and *Hadrodontina aequabilis* has three types of elements. Moreover, the *Scythogondolella* apparatus possesses element positional homologies shared by ozarkodinin, prioniodinin and prioniodontid conodonts, and the elements of the S_1 and S_2 positions are cypridodelliform and enantiognathiform in the superfamily Gondolelloidea. The *Hadrodontina aequabilis* apparatus has S_{1-2}, and P_{1-2} element types that differ from those in the gondolelloid apparatus, but it has the same extensiform digyrate morphotypes in both the S_1 and S_2 positions, and the angulate elements in positions of the P_1 and P_2.

In addition, many reported Triassic natural assemblages or clusters contain similar element morphologies and structures, which shows a great potential to reconstruct some new apparatuses. These include the Early Triassic *Hindeodus parvus* and *Clarkina* from China and Japan that were preserved as articulated assemblages in association with preservation of probable fossil conodont eyes on the bedding planes (Takahashi et al., 2019; Agematsu et al., 2017; Zhang et al., 2017). Additional natural assemblages contain *Neogondolella* from Monte San Giorgio, Switzerland (Goudemand et al., 2011; Orchard and Rieber, 1999; Rieber, 1980) and fused clusters of *Pseudofurnishius murcianus* from Slovenia (Kolar-Jurkovšek et al., 2018), both of which were discovered from Ladinian strata (Middle Triassic). Late Triassic (Norian or Rhaetian) fused clusters (formed by P elements or ramiform elements) and natural assemblages comprise *Mockina slovakensis*, *Misikella hernsteini*, *M. ultima* and *M. posthernsteini* from Italy and Hungary (Demo, 2017; Mastandrea et al., 1999, 1997; Roghi et al., 1995; Kozur, 1989; Budai and Kovács, 1986) and *Mockina* (and possibly *Parvigondolella*) from Baoshan, Yunnan Province, southwestern China (Zeng et al., 2021), some of which shared positional homologies elements in apparatus.

The composition of the *Nicoraella* apparatus has been discussed through discrete elements (Chen et al., 2019; Kolar-Jurkovšek et al., 2018; Huang et al., 2011; Sun et al., 2009; Kozur and Mock, 1991) and some fused clusters (Huang et al., 2019a, b), and its architectural model had been reconstructed by several relatively three-dimensional clusters (Huang et al., 2019c). Hence, the basic element compositions and architecture of the *Nicoraella* apparatus has been demonstrated previously. However, there still are some aspects need to be refined about the total number of apparatus composition and the accuracy of model architecture. Here we report several newly discovered natural assemblages from Luoping County, Yunnan Province, southwestern China (Fig. S1). Together with previously reported articulated fused clusters (Huang et al., 2019a, b), we measured the length of S_{2-4} elements as variables and discuss whether the size of these elements has any effect on the architecture of reconstructed apparatus. In other words, we attempt to explore if the architectures vary in different sized materials or the architecture of apparatus remains stable in the different growth staged materials. Furthermore, based on the previously reconstructed *Nicoraella* apparatus model (Fig. 1 in Huang et al., 2019c), we could calibrate the element positions
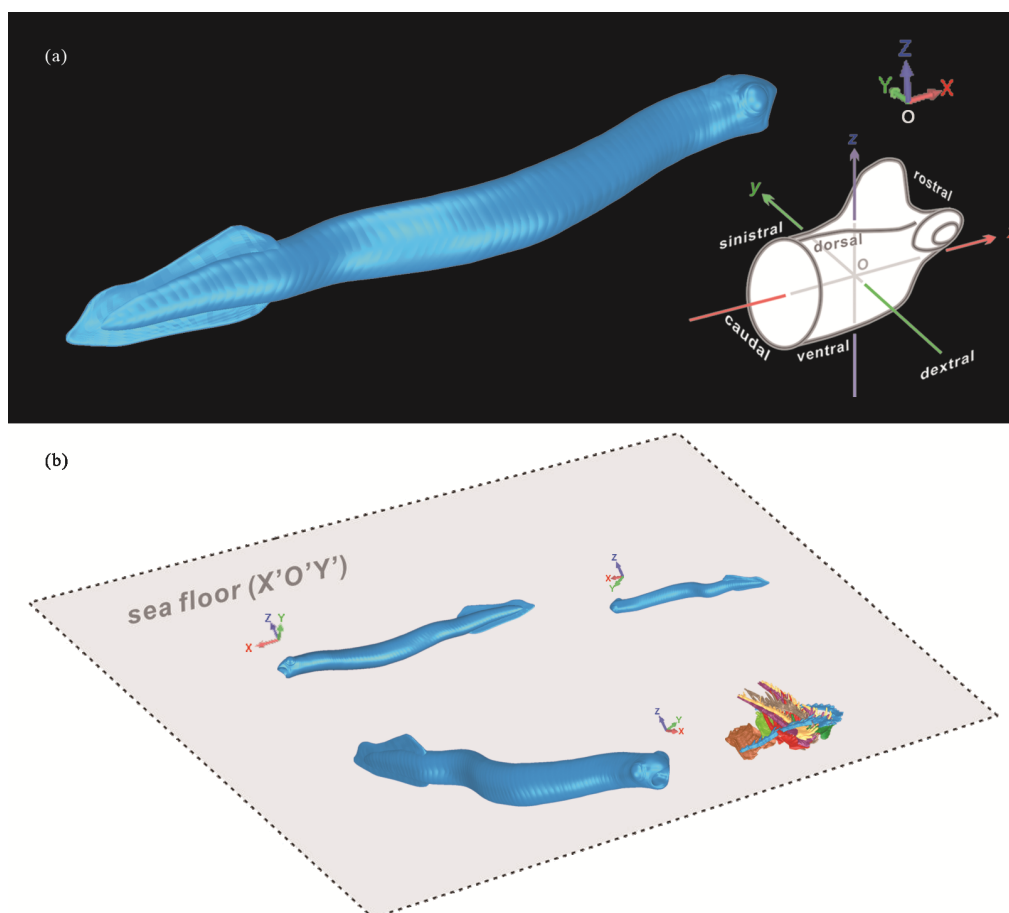
Figure 1. (a) Reconstruction of a sketch conodont animal with the defined Space Rectangular Coordinate System (SRCS); and (b) the biological orientations in conodont head with the different postures when their corpses fell on the sea floor ($X'O'Y'$).

of the S-M, P_2 and P_1 in the apparatus. The aim of this paper is to further adjust previous *Nicoraella* model on the basis of the new materials, acquiring a more precise architectural model, and lay a solid foundation for assessment of the architecture of apparatuses in the superfamily Gondolelloidea.

1 GEOLOGICAL SETTING

The Guanling Formation is widely distributed in western Guizhou and eastern Yunnan provinces. It bears the well-known Middle Triassic fossil Lagerstätten of the Luoping Biota (Hu et al., 2011) and Panxian Fauna (Jiang et al., 2009) in Member II of this formation. The Guanling Formation can be subdivided into two members (Zhang et al., 2009): Member I is about 333 m thick and composed of greyish muddy dolostone at the upper part, heterolithic colored mudstone and siltstone at the lower part, and the "green-bean rocks" (regional volcanic ash bed) as the marker bed separating Guanling Formation and the underlying Jialingjiang Formation (Yan et al., 2015). Member II is nearly 580 m thick and mainly consists of grey or dark muddy limestone, dolomitic limestone, nodular limestone, and micritic limestone with siliceous nodules (Zhang et al., 2009). The Luoping Biota occurs in the middle part of the Member II of the Guanling Formation. In particular, the biota was preserved in laminated micritic limestones with siliceous nodules and bands. The Luoping Biota includes lots of articulated fossils of vertebrates (marine reptiles, fishes, con-

odonts), arthropods (decapods, isopods, horseshoe crabs, thylacocephalas, millipedes), echinoderms (crinoids, sea cucumbers, sea stars, sea urchins, ophiuroids), molluscs (ammonites, bivalves, gastropods), brachiopods (lingulids), plants, and trace fossils (Huang et al., 2019a, b, 2011, 2010; Luo et al., 2019, 2018, 2017; Hu et al., 2017, 2011; Wen et al., 2013, 2012; Feldmann et al., 2012), marking the final recovery of marine ecosystem after the End-Permian Mass Extinction (Benton et al., 2013; Chen and Benton, 2012). These fossils were preserved in a relative deep water environment at the southwestern part of the Yangtze Platform near the Nanpanjiang Basin during the early Middle Triassic (Ma et al., 2021). The facies characteristics of the sedimentary macro-structures, microscopic features, geochemical proxies, fossils distribution and bioturbation evidences, indicate that the paleoenvironment of the Luoping Biota is an anoxic sedimentary environment (Fig. 2) (Ma et al., 2021; Luo et al., 2019) with the intermittent turbidity current and slump events (Bai et al., 2010; Huang et al., 2009). Microbial mats are suggested to play important roles in the fossilization of the Luoping Biota and the lime mud precipitation in strata (Luo et al., 2021, 2013).

2 MATERIALS AND METHODS
2.1 Terminology

The biological orientations of the apparatus in this study follow Purnell et al. (2000). According to the conodont soft ani-
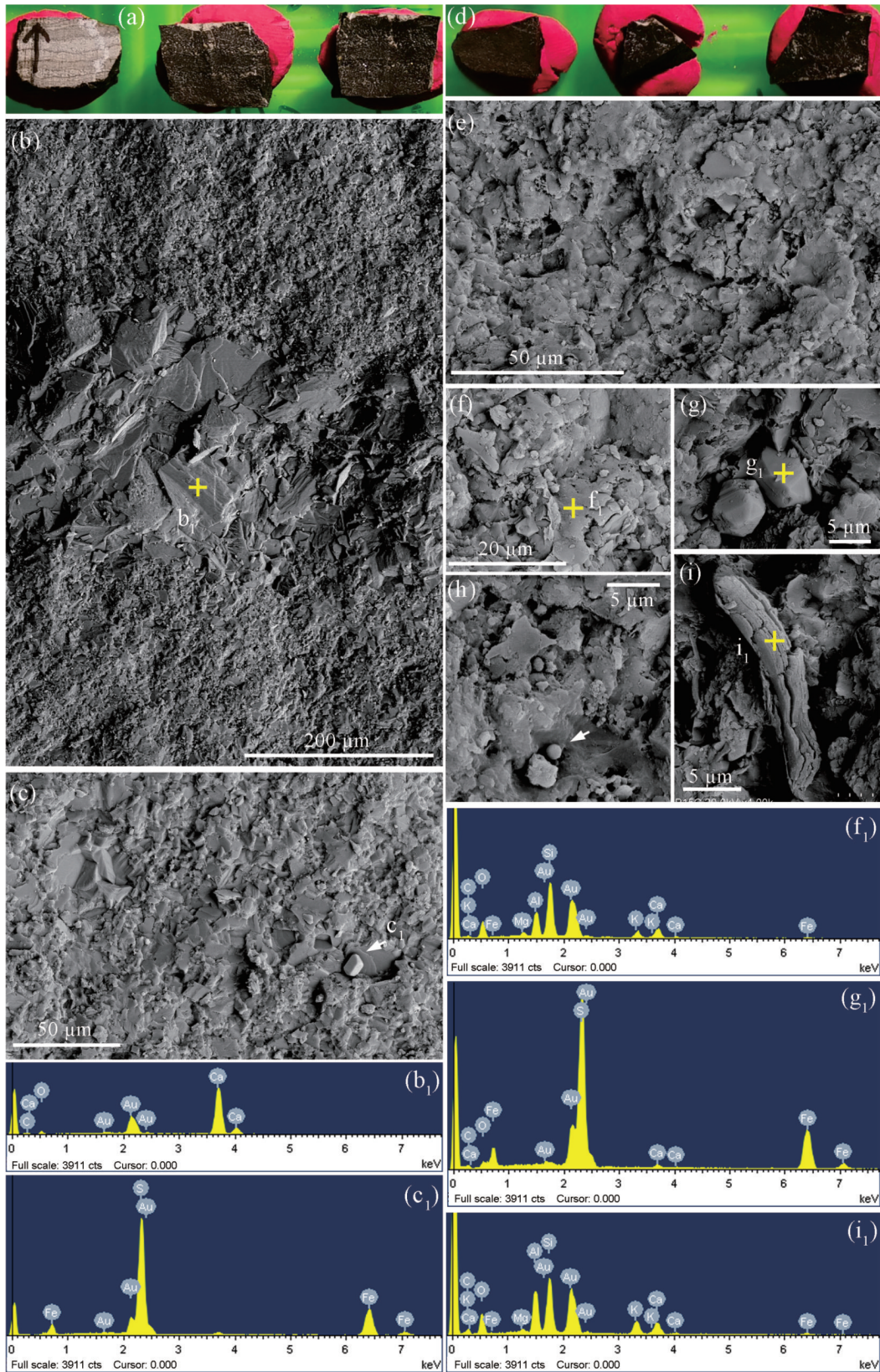
Figure 2. SEM photographs showing the mineral size stratification in the cross section of natural assemblage and the platy clay minerals on the tops of beds. samples are from the Bed 15 in the lower fossil layers of the Shangshikan Section. (a) Cross section of the natural assemblage samples. Clear laminated structures on the cutting surface of the left 1 sample; unclear structures on the surfaces of the fresh samples of the right 2–3. (b)–(c) Close-up of layers showing the size variation of the layers, the big calcite minerals at the middle (elements of EDS shown in b_1), relative small calcite minerals upper and below, a pyrite grain (ca. 5 μm length) in the small layers (elements of EDS shown in c_1). (d) The fresh samples of the bedding surface showing the clay minerals on the tops of beds (e)–(f), (i), elements are mainly composed of the Si, Al (f1), (i1), and some particles of the pyrite (g) and coccoidlike spheroids (h).

mal from Granton, Edinburgh, Scotland (Aldridge et al., 1993), they are named as rostral, caudal, sinistral, dextral, dorsal and ventral, respectively, corresponding to the anterior of head and the posterior of tail, left and right side of body, upper of back and lower of belly. We use traditional terms to denote the orientations of single elements and their processes ('oral', 'anterior', 'posterior', etc., with regard to their cusps). In order to simulate the final attitudes of the dead conodont animals lying on the sea floor, we erect a Space Rectangular Coordinate System (SRCS) (Fig. 1) following those in Purnell and Donoghue (1998) and Takahashi et al. (2019). As presented in Fig. 1a, the long axis of the conodont animal is designated as the X axis with respect to rostral-caudal direction, the Y axis to dextral-sinistral, and the Z axis to dorsal-ventral. These three axes are orthogonal to one another and intersect at point O, forming sagittal planes termed as XOY, XOZ and YOZ. The rostral, sinistral and dorsal orientations are assigned to the positive direction of the X axis, Y axis and Z axis, respectively, and the coordinate system obeys the right-hand rule. We assume that the sea floor is relatively parallel to its XOY plane when a living conodont animal was swimming in the sea, so we can call the sea floor as the $X'O'Y'$ plane to differentiate the plane of XOY. We use the same coordinate system for reconstruction of the conodont apparatus model in the software platform Geomagic Wrap 2015, and simulate the different attitudes of conodont apparatuses collapse on the sea beds when the conodont animals died.

2.2   Specimen Collections

The studied materials were all collected from Member II of the Guanling Formation at Shangshikan and Dawazi sections (near Dawazi Village, Luoping County), and Liziqing Section (Luxi County), Yunnan Province, southwestern China (Fig. S1). Here we report ten new conodont natural assemblages, labelled as LPNA1, LPNA2, LPNA3, LPNA4a, LPNA4b, LPNA5a, LPNA5b, LPNA6, LPNA7 and LPNA8, respectively (Figs. 3–7, S2–S4), from the Shangshikan Section. Samples were cut into small pieces and imaged using scanning electron microscope (SEM). All specimens were stored at the Chengdu Center, China Geological Survey. The articulated clusters for comparisons (Figs. S12–S13) have been documented previously (Huang et al., 2019a, b), and other unpublished clusters are described in the Electronic Supplementary Materials (ESM) data (Figs. S5–S7).

2.3   SEM and Stereomicroscope Photography

The highly compressed natural assemblages (Figs. 3–5, S2–S4) were photographed using the SU8010 Scanning Electron microscope (SEM) at the State Key Laboratory of Biogeology and Environmental Geology, China University of Geosciences (Wuhan). The fused clusters (Fig. S13) were scanned using the SEM (Quanta 200) at the State Key Laboratory Geological Processes and Mineral Resources, China University of Geosciences (Wuhan). The natural assemblages (Figs. 6b, 7) and fused clusters (Fig. S14) were scanned using the SEM (Hitach S-4800) at Chengdu Center of China Geological Survey. The natural assemblage in Fig. 6a was photographed using the Zeiss Smartzoom 5 in Chengdu Center, China Geological Survey.
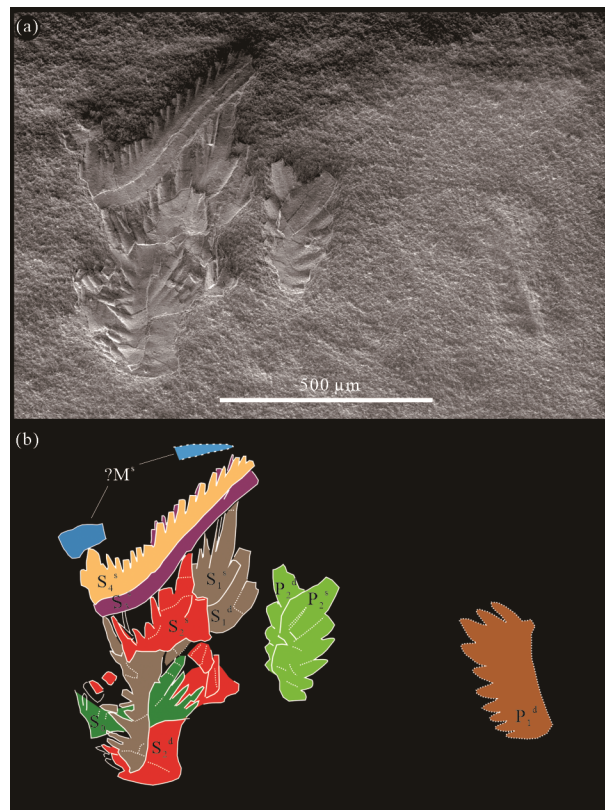

Figure 3. Articulated conodont natural assemblage from the upper fossil layers of the Shangshikan Section, as the SEM photograph (a) and interpretive drawings (b). Sample catalog number is LPNA4b. Scale bar is 500 μm. Brick red represents P_1 elements; chartreuse. P_2; green. S_0; brown. S_1; red. S_2; purple. S_3; orange. S_4; blue. M elements; respectively.

2.4   Synchrotron X-Ray Microtomography

The fused clusters (Figs. S5–S6, S12) were scanned employing the novel nondestructive technique of synchrotron-radiation X-ray tomography (SRXTM), with the beamline of the X02DA TOMCAT at the Swiss Light Source, Paul Scherrer Institute (Villigen, Switzerland). Slice data were analyzed using the software Avizo 8 and 9. Finally, the renderings were processed through the software Geomagic Wrap 2015 to adjust the digital three-dimensional apparatus and simulate collapse orientations.

2.5   Size Measurement of the Samples

In order to measure the size of specimens, we list the clusters and assemblages in one figure under the same scale (Fig. S9). The S_3 and S_4 elements are very similar with only slight differences in length of their anterior and posterior processes; so if they are scattered on a bedding surface, it is hard to differentiate them, thus they will be treated as an entirety of S_{3-4}. The S_4, S_3 and S_2 elements are the core part of the apparatus, and they are arranged successively inwards. The S_4 and S_3 elements are arranged outermost, and they are almost the longest elements in the apparatus, so we use their lengths to represent for the relative size of the apparatuses; if the S_{3-4} elements are lost or highly broken, we use the S_2 elements instead to evaluate the apparatus size.

Linear dimensions of the S_2, S_3 and S_4 elements were measured by ocular line proportion to a standard scale (micrometer)
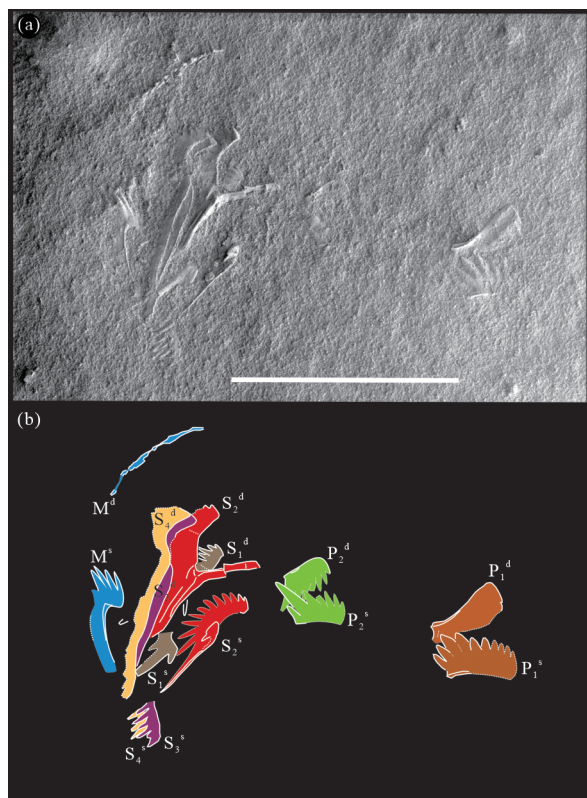
Figure 4. Articulated conodont natural assemblage from the upper fossil layers of the Shangshikan Section, as the SEM photographs (a) and interpretive drawings (b). Sample catalog number is LPNA5a. Scale bar is 1 mm. Color codings follow in Fig. 3.

Figure 5. Articulated conodont natural assemblage from the upper fossil layers of the Shangshikan Section, as the SEM photograph (a) and interpretive drawings (b). Sample catalog number is LPNA5b. Scale bar is 500 μm. Color codings follow in Fig. 3.

of the images using either Avizo or CorelDRAW 2018, as with all specimens from the Luoping Biota (Huang et al., 2019a, b). Here, we measure element linear dimensions as shown in Fig. S10, using the S_{3-4} element anterior and posterior process length, and S_2 element anterior process length. We use native program R to analyze the data and make result figures (Fig. S11).

2.6　Apparatus Repair

The new model was prepared by using cluster of pm028-18-wy1-C1 (Fig. S12a_1), which contains all 15 elements of the apparatus. This specimen was introduced in detail to reconstruct a new conodont apparatus of *Nicoraella* (Huang et al., 2019b, c). However, except for the P_1 elements, the other components are highly compressed or to some degree broken, which makes it hard to reconstruct a precise model. Therefore, we repaired each element of the apparatus on the basis of all characteristics of their positional homologous elements in our collection, and by using the software of Autodesk Maya.

3　RESULTS

3.1　Taphonomy of Conodont Natural Assemblages

In order to better understand the micro-environment around conodonts, here we observed the micro-structures of the samples that preserve the conodont natural assemblages in detail. The samples were cut into small pieces, with one showing the clear laminated layers in cross section (Fig. 2a). However it is hard to observe this pronounced characteristics in other
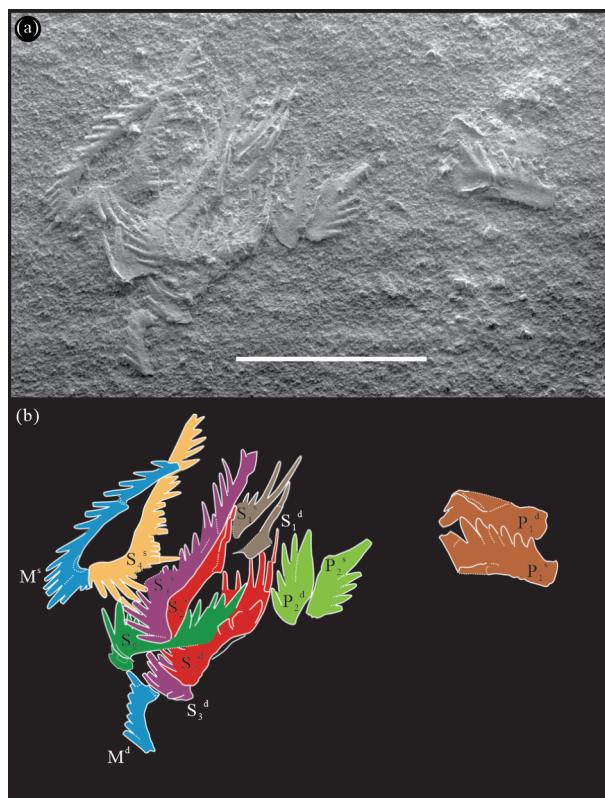
black background fresh samples. Of the weathered samples, it shows the grey coarse surface (Fig. S2) and yellowish thin laminated layers (Fig. S3). Under the SEM, the layered sample presents clearly different mineral sizes, the coarse layers have big mineral crystals (Fig. 2b), the upper and lower layers are relative small mineral granules (Fig. 2c), that are mainly comprised of calcite (Fig. $2b_1$). Although there are no clear clay minerals between the boundary of layers (Fig. $2b_1$) in the cross section, lots of platy clay minerals are observed on the tops of beds and oriented parallel to bedding surface (Figs. 2d – 2e); some blankets relatively angular grains and form small-scale wavy laminae (Figs. 2e–2f). EDS analysis indicates that those platy clay minerals are mainly composed of Si, Al, O (Figs. $2f_1$, $2i_1$), along with few C, K, Ca, Mg, Fe components. There are some other tiny objects such as coccoidlike spheroids (Fig. 2h) and pyrite grains (Figs. $2c_1$, $2g_1$). The microstructures on the surface of samples preserving with conodont natural assemblages, it could observe the laminal structures on the bed (Figs. S2a, S3a); the minerals are mainly composed of dolomites (Fig. $S2e_1$) and calcites (Fig. $S2e_2$), and irregular calcites are highly weathered (Fig. $S2e_2$), rhomb dolomites are weathering resistant. It is hard to diagnose the clay minerals on the weathered bedding surfaces, but it can be detected by EDS with the element peaks of Si and Al in context of the matrix (Figs. $S2e_3$, $S3c_{1-3}$ and $S3d_{1-4}$). EDS results on conodont natural assemblages exhibit high phosphorus peaks. Which is consistent with the apatite nature of conodonts (Figs. $S2b_1$, $S3b_1$, Sd_5). There are
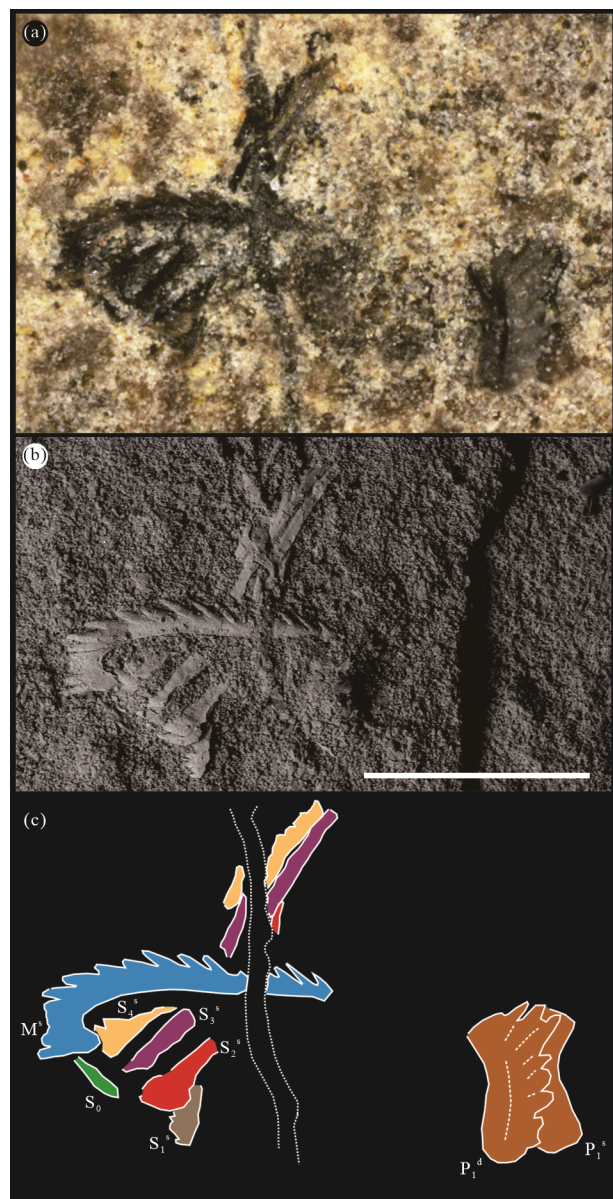
Figure 6. Articulated conodont natural assemblage from the lower fossil layer Bed 15 of the Shangshikan Section, as the stereo photograph (a), SEM photograph (b) and interpretive drawings (c). Sample catalog number is LP-NA6. Scale bar is 500 μm. Color coding is the same as in Fig. 3.

Figure 7. Articulated conodont natural assemblage from the upper fossil layers of the Shangshikan Section, as the SEM photograph (a) and interpretive drawings (b). Sample catalog number is LPNA8. Scale bar equals 500 μm. Color codings are the same as in Fig. 3.

no prominent characteristics of the testing samples, but there are some similar features as described by Luo et al. (2018) in the laminated limestones: "distinct in wavy laminated layers of dolomitic muddy limestone that are the feature of the Luoping reticulated ridge structures (microbial mats), thought to have played a crucial role in the preservation of the fossils through sealing and microbial coats". So, the characteristics in the laminated limestones could explain why they play an important role to well preserve the articulated conodont natural assemblages on the bed surfaces.

3.2   Components of Natural Assemblages

Ten new conodont natural assemblages have been found in the Luoping Biota, which were preserved as either articulated (Figs. 3–7) or scattered forms (Fig. S4). On the basis of previ-
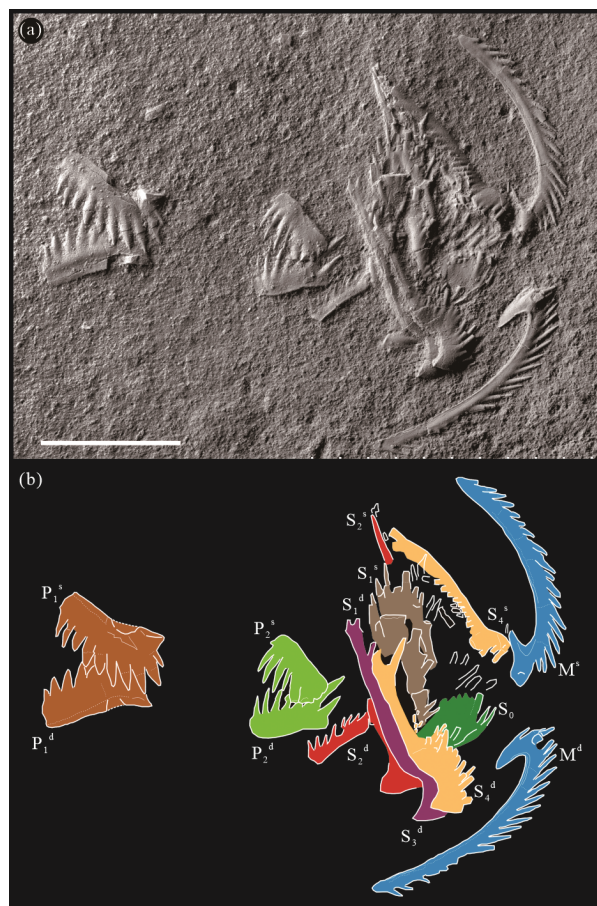
ously reconstructed *Nicoraella* apparatus (Huang et al. 2019a, b, c), it is easy to discern each component in a natural assemblage. The articulated assemblages are described as follows, with disarticulated ones described in supplementary materials.

Assemblage LPNA4b is composed of nine skeletal elements and two shallow imprints (Fig. 3), including seven S elements and a pair of P_2 elements, a possible sinistral M and P_1 element imprint, and P_1 element located far away from the S array. The S elements are placed rostrally immediately to a pair of occlusal P_2 elements. A possible sinistral M element remains a vague imprint and a small piece adhering to the cusp of the sinistral S_4 element; the S elements are more or less fragmentary, of which the sinistral S_4, S_3, S_2, S_1 and the middle S_0 elements are overlapped one by one; these S_4^s, S_3^s and S_0 elements are broken with their anterior processes, and the lateral process of S_2^s element is missing. The dextral S_1 and S_2 elements lie beneath the S_0 element. These interpretable elements are illustrated in Fig. 3b.

Assemblage LPNA5a has 13 elements (Fig. 4), including the paired P_1 and P_2 elements, seven S and two M elements. The P_1 and P_2 elements lie on the bedding surface with their opposing denticles; the occlusal paired P_2 elements are located much closer to the S array than the P_1 elements, as shown in Fig. 3, however most anterior parts of their denticles are

wrapped in matrix. Two M elements settle outside the S array. The dextral S_4, S_3, S_2, and S_1 elements are juxtaposed, with their denticles enclosed in the host rocks. The sinistral S_2 element only displays its inner-lateral process and part of the outer-lateral process. The anterior processes of the sinistral S_4 and S_3 elements are covered under the S array, and just their posterior part are exposed.

Assemblage LPNA5b possesses 14 elements (Fig. 5), the P_1 elements preserved oppositely each other with their denticles, and the P_2 elements located close to the rostral S array. The dextral and sinistral S_2, S_3 elements are aligned from the median region outwards to the S_0 elements. The dextral and sinistral S_1 elements just display their posterior processes, and their anterior processes are hidden under the sinistral S_{2-4} elements. The sinistral S_4 element is overlapped by the sinistral M element. The dextral M element may lose part of its long lateral process, and located rostro-ventral of the S array.

Assemblage LPNA6 contains seven elements (Fig. 6), i.e. a pair of P_1 elements located caudally, one element piled on the other, and a relative long distance from the S-M array. Two P_2 elements were not observed in this specimen. Six elements are identified as the S-M part, of which the distinct sinistral M element overlaps the incomplete sinistral S_{4-1} elements; S_0 element just has a small lateral process. A fissure traverses the S-M elements, forming a narrow gap.

Assemblage LPNA8 could identify fourteen elements (Fig. 7) with four parts, paired P_1 elements sit caudally showing a relatively long distance to S-M array, the sinistral element piled upon the dextral element with an acute angle, and two P_2 elements located caudally near by S-M group, and also the sinistral element piled on the dextral element with an acute angle as like the P_1 elements. The dextral S_{2-4} and sinistral S_4 elements are easy to identify with their shapes, however there are some broken elements in the inner part of S group, but we could recognize these elements of S_0, $S_1^{s,d}$ and S_2^d by their distinctively outlines. The conspicuous, completely sinistral and dextral M elements laid outside and slightly rostral to S elements, and formed a regular arc as like in the cluster of Fig. S12d.

Conodont clusters All clusters in Figs. S12–S13 have been illustrated in previous work (Huang et al., 2019a, b, c), and the new clusters in Figs. S5–S7 are described in the ESM data. The cluster in Fig. S12a (pm028-18-wy1-C1) has 15 fused elements, including a single and seven paired elements (4P-2M-9S). This cluster contains each component of the *Nicoraella* apparatus, and the reconstructed model is based on this specimen in this paper.

3.3 Size of the Apparatus

The elements size in a conodont apparatus could be used to assess the relative size of a conodont animal, and vice versa. Large animals should possess large apparatuses consisting of large elements (Aldridge et al., 1993), and this viewpoint was verified from measurements of five relatively complete fossil conodont animals (Purnell, 1994). Purnell (1994) analyzed the lengths of P, M and S elements of Carboniferous natural assemblages of *Idiognathodus* and *Gnathodus bilineatus* to assess the relative ontogeny of the element, and found that the Pa (P_1) ele-

ments have slight positive allometry in their platform with respect to their length. This conformed with predictions of the tooth function, and then the length of Pa (P_1) element was used as a proxy to assess relative growth size of an apparatus. With respect to the Pa (P_1) element, the M element showed negative allometry and the Pb (P_2) and S elements were isometry. So, this enables us to use the S elements to estimate the relative size (big or small) of the apparatus.

The uniformly scaled fused clusters and natural assemblages (Fig. S9) have three size levels (small, medium, large). Of them, cluster 3 (scanned by SEM), cluster 5 (scanned by CT) and assemblage 2 (SEM) are small apparatuses. Cluster 15 (SEM), cluster 1 (CT) and assemblage 6 are large apparatuses. Based on quantiles of S_{2-4} element lengths, we identify mean lengths of small (<513 μm), medium (513–593 μm), and large (>593 μm) for S_4 elements; small (<550 μm), medium (550–646 μm), and large (>646 μm) for S_3 elements; and small (<183 μm), medium (183–197 μm), and large (>197 μm) for S_2 elements. These data are summarized in Table S1.

According to these size ranges, it is easy to distinguish their relative size and architecture from synchrotron scanned images, and their patterns of overlap and positions of homologous elements (Huang et al., 2019b). These characteristics can also be tested from the SEM images (Huang et al., 2019a). Although we could not observe the whole elements in the natural assemblages, we can distinguish the patterns of elements overlap from one side of the apparatuses, which show that homologous elements sit in the same positions, and do not change with different apparatuses sizes. In summary, the architecture of the apparatus does not change with the variation of element sizes. Thus, we believe that we can establish a reliable architectural model based on the different sized specimens, no matter the state of preservation of fused clusters or natural assemblages.

3.4 Calibrated Apparatus Architecture

Following the biological orientations and anatomical notations of the conodont apparatus (Purnell et al., 2000), the S-M elements are placed rostrally, the P_{1-2} elements are set caudally to the S-M array, with bilaterally symmetrical structure of sinistral and dextral side that appears in many three-dimensional clusters. Along with the newly discovered natural assemblages, the architecture of the *Nicoraella* apparatus (Fig. 1 in the Huang et al., 2019c) could be further refined. As shown in Fig. 8, the paired S_{1-4} and M elements symmetrically flank both sides of the *XOZ* sagittal plane. The S_0 element is located in the middle of the S_{1-4} elements with its long process ca. 25° to the *X* axis in the *XOZ* plane, and its two lateral processes slightly protrude rostrally of the S_{1-4} elements. The long processes of the S_{1-4} elements incline slightly inward to the *XOZ* plane and point to dextro-dorsal and sinistro-dorsal, respectively: their lower margins juxtaposed approximately parallel to one another, with these lower margins at ca. 60° relative to the horizontal *XOY* plane. The posterior denticles and cusps of the S_{1-4} elements are oriented caudo-dorsally, with their cusps more caudal than their rostral processes. The M elements are placed at the outside of S elements with their long posterior processes ca. 60° relative to the *XOZ* plane and almost parallel to the horizontal *XOY* plane. They located at mid-height of the S ele-
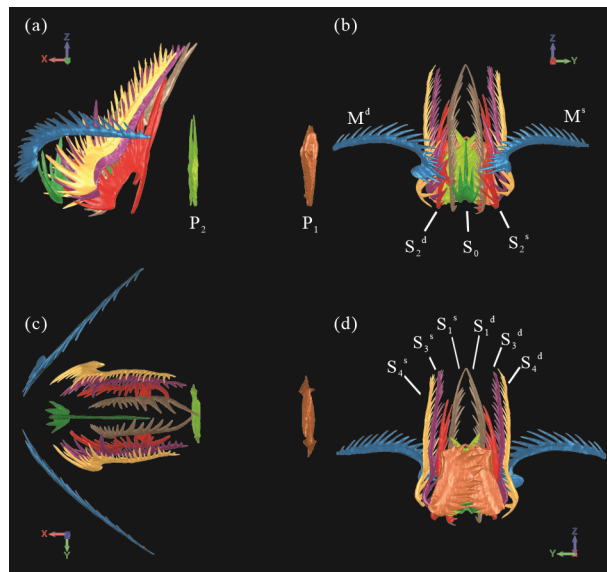
Figure 8. Orientations of the recalibration model of the *Nicoraella* conodont apparatus. (a) Sinistral view of the apparatus, P_2 elements locate close to S array, P_1 elements are much far, the sinistral elements lay behind of dextral P elements; (b) rostral view; (c) dorsal view; (d) caudal view, with the notations of the S-M array, and showing the anatomical notation of the dextral and sinistral S_2–S_4 and M elements. Color coding is the same as in Fig. 3.

ments with their short processes, and project slightly beyond the S_0 element when viewed dextrally and sinistrally. The flat surfaces of the blade shaped P elements are oriented parallel to the sagittal plane of the *YOZ*. The anterior part of the P elements are located slightly higher than the lower margins of the S-M array on the *Z* axis (dorso-ventral axis) in the *YOZ* plane, and they are occluded with an acute angle and their dextral elements positioned rostrally to their sinistral pair. The P_2 elements lie close to and below the distal of S elements, approximately halfway between the rostral limit of the S-M array and the P_1 elements along the *X* axis. The P_1 elements are settled caudally away from the P_2 and S-M elements.

The new model of *Nicoraella* (Fig. 8) has several differences when compared with our previous reconstruction (Fig. 1 in the Huang et al., 2019c). Changes are: (1) The S_0 element is more protruding rostrally the S_{1-4} elements; (2) the M elements are at a slightly larger angle (ca. 5° more) to the S elements, and their long posterior processes almost parallel to the horizontal plane; (3) the S_{1-4} elements are at a slightly larger angle (ca. 5° more) to the horizontal plane; (4) the P_1 and P_2 elements located lower to mid-height of the S array and occluded with an acute angle, especially the P_1 elements positioned more caudal than our previous interpretation. We can test this new model in the following ways.

3.5   Apparatus Collapse Simulations

The fossils of conodont natural assemblages could preserve their original architectures under conditions of no transport, fast burial and exceptional environments. Different attitudes of dead conodont animals would produce different postures of the apparatus collapses on sea floor (Purnell and Donoghue, 1998), and the arrangements of natural assemblages or

clusters could reflect the attitudes of the dead animals (Purnell and Donoghue, 1998; Aldridge et al., 1987; Briggs and Williams, 1981). In order to comprehend the establishment of the final attitudes and the process of apparatus collapse, we use the SRCS and physical modelling method (Purnell and Donoghue, 1997) to test the validity of our architectural model by viewing from different perspectives.

In our collections, the S elements (S_0 and S_{1-4} elements) are a relatively stable group, and they have constant component elements in fused clusters and natural assemblages. The M elements usually exhibit different postures in the clusters and assemblages, seemingly controlled by a different muscle system to S elements group. P_1 and P_2 elements are other two groups, controlled by independent muscle system. They lie far away from the S-M elements, and often occur in bedding plane assemblages, but rarely fused together with clusters of S and M elements (Zeng et al., 2021; Huang et al., 2019a). Conodont apparatus collapse is a complicated process, which may be affected by the degree of soft tissue decomposition, the compaction effects in diagenesis, and the eel-like, elongate and laterally compressed body shapes. Especially, the laterally compressed body shapes produced a number of lateral side postures far beyond other orientations (Purnell and Donoghue, 1998). Here, the revised *Nicoraella* model was first considered with reference to the collapse orientations of the S elements, and further used the M and P elements to constrain the final postures.

The first articulated assemblage (LPNA4b) preserves three parts that are highly compressed (Fig. 3), and these can be replicated by viewing the model from sinistro-ventral with slightly rostral (Fig. $9a_{2-3}$). This orientation effectively simulates the overlap among the ramiform S elements array, P_1 and P_2 elements, the seemingly 'parallel' arrangement of the broken S elements, the shallow imprint of the sinistral M element addressed on the S_{3-4} elements, the P_2 elements immediate to the S array, and the P_1 elements a little further away from the S elements. Detailed differences between the model and this assemblage, including the separation of P_2 and S elements, can be rationalized by rotating elements during collapse of the three-dimensional arrangement of the elements in the model to the two-dimensional plane. It is hard to test the orientations of M elements as they are missing in this assemblage.

The second assemblage (LPNA5a) contains four parts that are also highly compressed (Fig. 4), including two arched M elements, an oblique S array, and paired opposed blade-shaped P_2 and P_1 elements (Fig. $9b_1$). This 'oblique' arrangement can be simulated by viewing the model from the dextro-dorsal perspective with caudal component (Fig. $9b_{2-3}$). In this orientation, the model could be accurately reproduced the positions of the rostral arched M elements and the overlaps of the dextral S and P elements. Minor differences between the arrangement of elements in the model and the assemblage are the narrow separation of the P_1 and P_2 elements, and slight deviation in directions of the distal parts of the dextral and sinistral S elements. These minor differences can be produced under the compaction effects during diagenesis.

The third assemblage (LPNA5b) includes four parts that are highly compressed (Fig. 5) than in the previous two assemblages, which preserves a parallel arrangement of dextral and
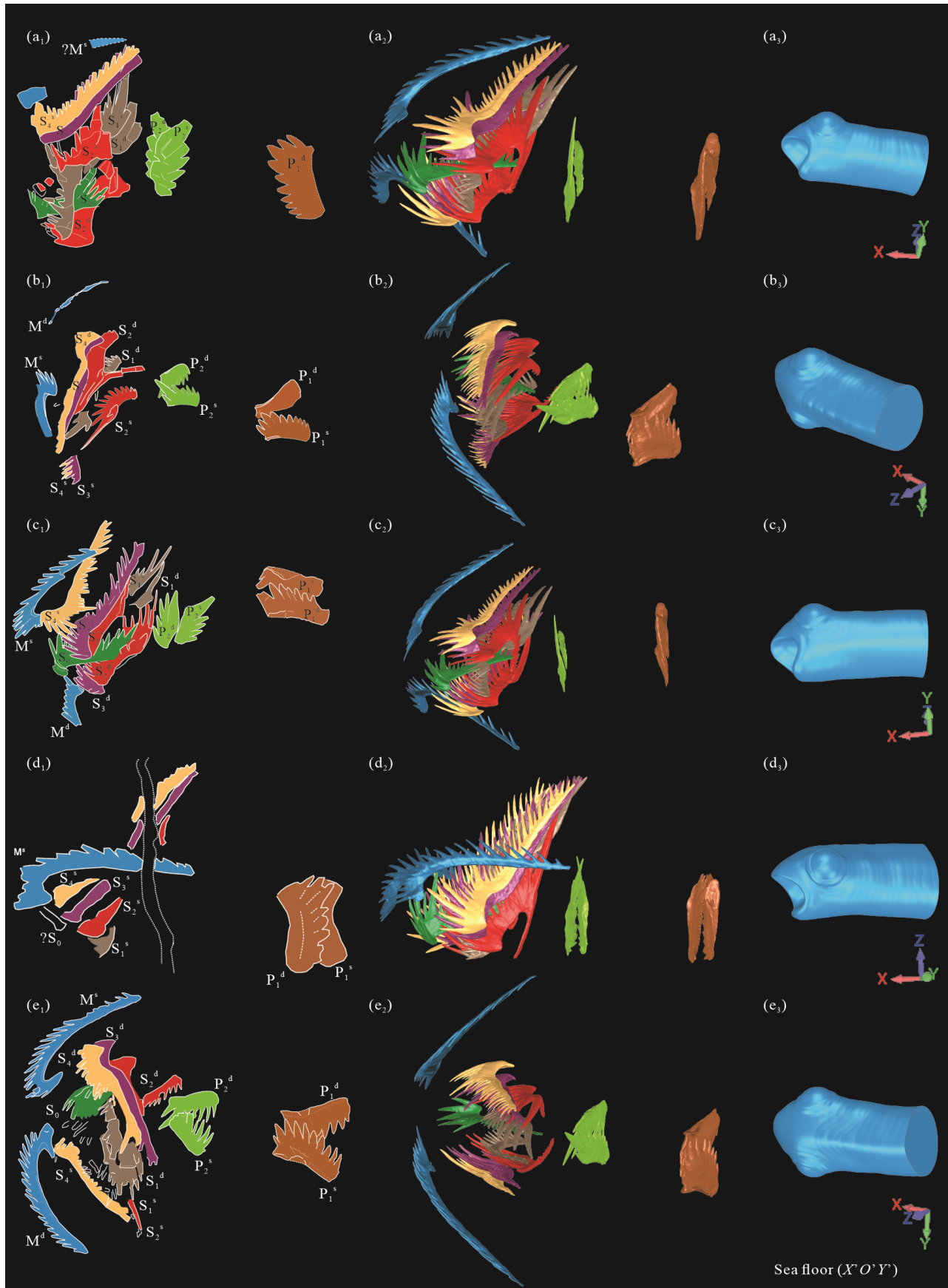
Figure 9. The simulated collapse orientations of the reconstructed apparatus for natural assemblages (columns 1 and 2), and the orientations of conodont animals with respect to collapse on sea floor ($X'O'Y'$) (column 3). Color coding is the same as in Fig. 3.

sinistral S_{2-3} elements, and paired adjacent P_2 and distant P_1 elements with respect to the S array (Fig. $9c_1$). This arrangement can be replicated by viewing the model from the sinistro-ventral side with a minor rostral component (Fig. $9c_{2-3}$). In this direction, we can effectively simulate the arrangement of S elements, and the relative positions of the M and P_{1-2} elements. In detail, a short process of the dextral M element is adpressed to the dextral S_3 elements, which could happen when the dextral M element broke in collapse. The sinistral S_4 element perhaps move away from the S array during collapse. Although the P_1 and P_2 elements are located in appropriate positions relative to the S array in the modeling simulation, they are not fully exact to the final orientations; the P_2 elements are separated with opposed orientation of their denticles, and the P_1 elements are rotated to the dorsal side in the assemblage. However, these minor changes possibly happened in collapse, and could occur when the P_2 elements separated and the P_1 elements rotated dorsally during soft tissue degradation.

The fourth assemblage (LPNA6) contains only the sinistral S and paired P_1 elements, with the dextral S counterpart may be covered by the matrix, and the P_2 elements are missing (Fig. 6). The sinistral M element piles upon the sinistral S elements at approximately 60° to the long process of the S_{3-4} elements, and the P_1 elements settle far away from the S-M series. This arrangement can be simulated by viewing the model from the sinistral side, with minor rostral and dorsal components (Fig. $9d_{2-3}$). In this orientation, the sinistral S-M elements perfectly match the overlap pattern, and the P_1 element arrangement is replicated with just slight gravitational rotation during diagenesis. Because the P_2 elements are missing in the assemblage, their positions cannot be further considered.

The fifth assemblage (LPNA8) possesses distinct four parts of the M, S, P_1 and P_2 (Fig. 7), the M and P_2 elements are relatively close to S array, P_1 elements locate caudally far away from S series. Two M elements present an arched shape with ca. 60 degrees by their long processes to X axis, both of the sinistral and dextral P_1 and P_2 elements have an acute angle, and the sinistral element piles upon the dextral one. This arrangement could be simulated by viewing the model from a slight oblique dorso-ventral orientation with minor dextral and caudal components (Fig. $9e_{2-3}$). In this orientation, the model accurately reproduces the positions of the rostral arched M elements, the overlaps of the dextral S_{2-4} elements, and the opposed P_1 and P_2 elements. Minor differences between the simulated model and assemblage are the S_1 and S_4^s elements, they slightly deviate the positions. These minor differences can be produced during apparatus collapse from three dimensional to the two dimension plane when diagenesis.

The fused clusters in Figs. S12–S13 were described in detail and discussed in our previous studies (Huang et al., 2019a, b), and the Fig. S14 is described in detail in the ESM. Most of these clusters are highly compressed and few of them have three-dimensional structures (Huang et al., 2019b). The majority retain S and M elements after acid digestion, and only a few clusters contain both P and S-M elements. The clusters in Fig. S12 were used to simulate collapse orientations (Huang et al., 2019c). Here we test the collapse orientations of the fused clusters again, and together with the newly reported clusters to vali-

date our new architectural model as shown in ESM Part C.

In summary, based on all of the orientations mentioned above, we can observe a similarity of the P elements, that they are isolated from the S-M array, and usually difficult to fuse together with the S-M elements during diagenesis, except the condition enclosing by massive matrix. Owing to characteristics of the P elements are separated from the S-M elements in the apparatuses, that's why we mostly only acquired P elements pair or S-M element clusters after acid digestion, and just few materials simultaneously contain P and S-M elements. S-M elements are more stable groups that share the same structures and the pattern of the elements arrangement from inner to outside. The P and M elements have many postures in the clusters and natural assemblages, however, we couldn't simulate all orientations of elements in samples through our reconstructed model using the physical modeling method. This situation is also appearance in the process of the Carboniferous *Idiognathodus* apparatus reconstruction (Purnell and Donoghue, 1998, 1997). So, it means the processes of the apparatuses collapse are more complicated, not simply view a three-dimensional apparatus from a direction to produce a stereo apparatus as a two-dimensional assemblage. It can speculate that the final postures of the natural assemblages are affected by many unknown factors after conodont animals dead during the diagenesis, but it is pity that we know little about details in those factors.

4   DISCUSSION

Combining recognitions from previously reported isolated elements, and fused clusters with information from the new natural assemblages, the *Nicoraella* apparatus can be finally confirmed by having a standard 15-element plan (9S-2M-4P). This result conforms to the apparatuses of ozarkodinin and prioniodinin conodonts, i. e., *Idiognathodus*, *Hindeodus*, *Clarkina*, *Gondolella*, *Scythogondolella* (Sun et al., 2021; Takahashi et al., 2019; Agematsu et al., 2017; von Bitter and Merrill, 1998; Purnell and Donoghue, 1997). The *Nicoraella* apparatus shows a $1S_0$-$8S_{1-4}$-2M skeleton pattern from the three-dimensionally fused clusters (Huang et al., 2019b), which can be validated from the new natural assemblages (Figs. 3–7). The four P elements of *Nicoraella* apparatus have been proposed before based on the discrete elements (Sun et al., 2009) and a 'complete' fused cluster (Fig. 9a, Huang et al., 2019b, c). However, it is difficult to determine their accurate numbers because all discrete elements and fused clusters are dissolved from host rocks, thus P elements are very easily lost in the extraction processes. This is why most clusters usually retain the S-M elements, with just a few P elements fused by the matrix to S-M array (Huang et al., 2019a, b, 2010). Thanks to the newly collected natural assemblages, here we can finally confirm that there are only four P elements in *Nicoraella* apparatus formed by paired P_1 and P_2 elements, respectively.

The gondolelloid apparatuses share the same component numbers (15 elements), the similar morphologies and element positional homologies, e. g., *Gondolella* (von Bitter and Merrill, 1998; von Bitter, 1976), *Neogondolella* (Goudemand et al., 2011), *Novispathodus* (Goudemand et al., 2012, 2011), *Nicoraella* (Huang et al., 2019a, b), *Pseudofurnishius murcianus* (Kolar-Jurkovšek et al., 2018; Ramovš, 1978, 1977), and

Mockina (Zeng et al., 2021; Demo, 2017). The elements in the S_1 and S_2 positions have been confirmed as the cypridodelliform (or grodelliform) and enantiognathiform elements, respectively. It is further implied that these apparatuses above have closely phylogenetic affinity and probably possessed a similar apparatus architecture.

Although the *Nicoraella* apparatus has been established based upon some three-dimensional fused clusters in our previous work (Huang et al., 2019c), its precise architecture still needs to be improved due to the fused clusters will unavoidably lose some information of the architecture in the process of the acid dissolution. Fortunately, the natural assemblages could make up for this deficiencies. Here we combine all information from the fused clusters and natural assemblages to show that small and large specimens possess the same overlap arrangement and structure of the apparatus. Thus, we could use all the samples to reconstruct a more reliable model using physical modelling method (Figs. 8, 9). Generally, the newly adjusted model (Fig. 8) has the same frame to other ozarkodinin apparatus, with a bilateral symmetrical structure, M elements are outermost of the S elements, S_0 element is situated at the middle of the S elements, and the P elements are placed caudally to S-M array. However, the positions of P and S-M array elements are somewhat changed in the new model regarding to the former one. It was hard to precisely evaluate their relative positions of the P_2 and P_1 elements with respect to S elements in previous fused clusters, because most of P elements are lost, or highly compressed, or fused together with S elements, but here their positions could be accurately determined on the basis of each element location in the natural assemblages. As shown in both of clusters and natural assemblages, the P_2 elements are close to S elements and they are positioned below the caudal 'posterior' tips of the S_{3-4} elements. Unlike the P_2 elements, limited evidence from fused clusters shows that the P_1 and S-M elements are sometimes fused together, meaning that the P_1 elements may locate much close to S array in the physical model, or have collapsed forward towards the S array during diagenesis. In fact, now it seems that all P_1 elements are situated farther in natural assemblages than clusters, suggesting P_1 elements are actually far away from S-M elements. In the refined model, the P_1 elements are approximate twice the distance from the rostral S array than the P_2 elements (Fig. 8). This marks a slight change in the P_1 element position, a little farther than previous reconstructed model (Fig. 1 in Huang et al., 2019c).

Compared to the earlier reconstructed S-M array (Fig. 1 in Huang et al., 2019c), the S_0 element has a slightly smaller angle to the *X* axis and places more rostrally to the S_{1-4} elements, the S_{3-4} elements are located a little farther from the S_2 elements, the M elements are slightly broader than before (Fig. 1 in Huang et al., 2019c), and their long posterior processes almost parallel to the horizontal plane (Fig. 8). It should be noted that the M pair are relative independent, and their various postures in the natural assemblages and clusters (Figs. 3–7, S12–S14), indicating that they may be controlled by a different musculature system to S elements.

Obviously, the clusters represent a narrow range of collapse orientations in which the elements overlap (Fig. S12a₁—high angles of collapse), so the previous model was not precise

sufficiently. Here the new assemblages are more informative about the relative position of the elements in that they represent a broader range of collapse orientations including those at a low angle of collapse, thus providing far better constraint on position of the P to S elements. Therefore, we have a more accurate model on the basis of all materials with natural assemblages and clusters.

5 CONCLUSIONS

Ten conodont natural assemblages together with the previously described fused clusters were collected from the Middle Triassic Luoping Biota in Yunnan Province, Southwest China. They preserve the original arrangement of the apparatus, showing direct evidence of the numbers and relative positions of all elements in the *Nicoraella* apparatus. Integrating all evidence from articulated natural assemblages, fused clusters, accumulations of bedding plane elements, and discrete elements described by Huang et al. (2011) suggests that the conodont *Nicoraella* is a 15-element apparatus, including nine S elements (single S_0, and paired S_1, S_2, S_3, and S_4 elements) and two M elements forming as a rostral 'grasping' array, and together with the paired P_2 and P_1 elements consist of the caudal 'cutting' groups. Fifteen elements in the apparatus is a conservative number in ozarkodinin apparatus over more than 250 million years evolution from the Ordovician to Triassic.

Analysis of different sized specimens reveals that the apparatus retains the same architecture through all staged ontogenies. Thus, the characteristics of conodont natural assemblages with different growth stages can be used to reconstruct a reliable architecture of the apparatus. All specimens demonstrate that the skeletal architecture is bilaterally symmetrical with a regular arrangement of the elements, and natural assemblages indicate the relative positions of each S-M component in the apparatus, where P_2 elements are closer to the S-M array, P_1 elements are more caudal than P_2 elements at twice distance as the limit of the rostral S elements. Finally, an accurate architectural model of the three-dimensional apparatus of *Nicoraella* was validated through simulating the different collapse patterns on the basis of natural assemblages and fused clusters.

Electronic Supplementary Materials: Supplementary materials Part A Figs. S1–S14 and Table S1; Part B Specimens De-

scriptions; Part C Apparatus Collapse Simulations for Clusters are available in the online version of this article at https://doi.org/10.1007/s12583-022-1793-z.

Conflict of Interest

The authors declare that they have no conflict of interest.

REFERENCES CITED

Agematsu, S., Uesugi, K., Sano, H., et al., 2017. Reconstruction of the Multielement Apparatus of the Earliest Triassic Conodont, *Hindeodus parvus*, Using Synchrotron Radiation X-Ray Micro-Tomography. *Journal of Paleontology*, 91(6): 1220–1227. https://doi.org/10.1017/jpa.2017.61

Aldridge, R. J., Briggs, D. E. G., Sansom, I. J., et al., 1994. The Latest Vertebrates are the Earliest. *Geology Today*, 10(4): 141–145. https://doi.org/10.1111/j.1365-2451.1994.tb00891.x

Aldridge, R. J., Briggs, D. E. G., Smith, M. P., et al., 1993. The Anatomy of Conodonts. *Philosophical Transactions of the Royal Society B Biological Sciences*, 340(1294): 405–421. https://doi.org/10.1098/rstb.1993.0082

Aldridge, R. J., Murdock, D. J. E., Gabbott, S. E., et al., 2013. A 17-Element Conodont Apparatus from the Soom Shale Lagerstätte (Upper Ordovician), South Africa. *Palaeontology*, 56(2): 261–276. https://doi.org/10.1111/j.1475-4983.2012.01194.x

Aldridge, R. J., Smith, M. P., Norby, R. D., et al., 1987. The Architecture and Function of Carboniferous Polygnathacean Conodont Apparatuses. In: Aldridge, R. J., ed., Palaeobiology of Conodonts. Ellis Horwood Press, Chichester. 63–75

Aldridge, R. J., Theron, J. N., 1993. Conodonts with Preserved Soft Tissue from a New Ordovician *Konservat-Lagerstätte*. *Journal of Micropalaeontology*, 12(1): 113–117. https://doi.org/10.1144/jm.12.1.113

Bai, J. K., Zhang, Q. Y., Yin, F. G., et al., 2010. Preliminary Study of Taphonomic Environment of Luoping Biota: Evidence from Sedimentary Structures. *Acta Sedimentologica Sinica*, 28(4): 762–767 (in Chinese with English Abstract)

Benton, M. J., Zhang, Q. Y., Hu, S. X., et al., 2013. Exceptional Vertebrate Biotas from the Triassic of China, and the Expansion of Marine Ecosystems after the Permo-Triassic Mass Extinction. *Earth-Science Reviews*, 125: 199–243. https://doi.org/10.1016/j.earscirev.2013.05.014

Briggs, D. E. G., Clarkson, E. N. K., Aldridge, R. J., 1983. The Conodont Animal. *Lethaia*, 16(1): 1–14. https://doi.org/10.1111/j.1502-3931.1983.tb01993.x

Briggs, D. E. G., Clarkson, E. N. K., 1987. An Enigmatic Chordate from the Lower Carboniferous Granton 'Shrimp-Bed' of the Edinburgh District, Scotland. *Lethaia*, 20(2): 107–115. https://doi.org/10.1111/j.1502-3931.1987.tb02027.x

Briggs, D. E. G., Williams, S. H., 1981. The Restoration of Flattened Fossils. *Lethaia*, 14(2): 157–164. https://doi.org/10.1111/j.1502-3931.1981.tb01918.x

Budai, T., Sándor, K., 1986. A Rezi Dolomit Rétegani Helyzete a Kezthelyi-Hegységben. *M Áll Foldtani Intézet Évi Jelentése Az*, 1984: 175–189

Chen, Y. L., Scholze, F., Richoz, S., et al., 2019. Middle Triassic Conodont Assemblages from the Germanic Basin: Implications for Multi-Element Taxonomy and Biogeography. *Journal of Systematic Palaeontology*, 17(5): 359–377. https://doi.org/10.1080/14772019.2018.1424260

Chen, Z. -Q., Benton, M. J., 2012. The Timing and Pattern of Biotic Recovery Following the End-Permian Mass Extinction. *Nature Geoscience*, 5(6): 375–383. https://doi.org/10.1038/ngeo1475

Demo, F., 2017. Analysis of Synchrotron Microtomography 3D Images of Exceptional Fused Cluster of Mockina Slovakensis (Conodonts): [Dissertation]. Università degli Studi di Padova, Padua. 63

Donoghue, P. C. J., Purnell, M. A., Aldridge, R. J., et al., 2008. The Interrelationships of 'Complex' Conodonts (Vertebrata). *Journal of Systematic Palaeontology*, 6(2): 119–153. https://doi.org/10.1017/s1477201907002234

Feldmann, R. M., Schweitzer, C. E., Hu, S. Q., et al., 2012. Macrurous Decapoda from the Luoping Biota (Middle Triassic) of China. *Journal of Paleontology*, 86(3): 425–441

Goudemand, N., Orchard, M. J., Tafforeau, P., et al., 2012. Early Triassic Conodont Clusters from South China: Revision of the Architecture of the 15 Element Apparatuses of the Superfamily Gondolelloidea. *Palaeontology*, 55(5): 1021–1034. https://doi.org/10.1111/j.1475-4983.2012.01174.x

Goudemand, N., Orchard, M. J., Urdy, S., et al., 2011. Synchrotron-Aided Reconstruction of the Conodont Feeding Apparatus and Implications for the Mouth of the First Vertebrates. *Proceedings of the National Academy of Sciences of the United States of America*, 108(21): 8720–8724. https://doi.org/10.1073/pnas.1101754108

Higgins, A., 1983. Carboniferous Fossils: The Conodont Animal. *Nature*, 302(5904): 107. https://doi.org/10.1038/302107a0

Hu, S. X., Zhang, Q. Y., Chen, Z. Q., et al., 2011. The Luoping Biota: Exceptional Preservation, and New Evidence on the Triassic Recovery from End-Permian Mass Extinction. *Proceedings of the Royal Society B*: *Biological Sciences*, 278(1716): 2274–2282. https://doi.org/10.1098/rspb.2010.2235

Hu, S. X., Zhang, Q. Y., Feldmann, R. M., et al., 2017. Exceptional Appendage and Soft-Tissue Preservation in a Middle Triassic Horseshoe Crab from SW China. *Scientific Reports*, 7: 14112. https://doi.org/10.1038/s41598-017-13319-x

Huang, J. Y., Zhang, K. X., Zhang, Q. Y., et al., 2009. Conodonts Stratigraphy and Sedimentary Environment of the Middle Triassic at Daaozi Section of Luoping County, Yunnan Province, South China. *Acta Micropalaeontologica Sinica*, 26(3): 211–224 (in Chinese with English Abstract)

Huang, J. Y., Zhang, K. X., Zhang, Q. Y., et al., 2010. Discovery of Middle Triassic Conodont Clusters from Luoping Fauna, Yunnan Province. *Earth Science—Journal of China University of Geosciences*, 35(4): 512–514 (in Chinese with English Abstract)

Huang, J. Y., Zhang, K. X., Zhang, Q. Y., et al., 2011. Advance Research of Conodont Fauna from Shangshikan and Daaozi Sections in Luoping Area, Yunnan Province. *Geological Science and Technology Information*, 30(3): 1–17 (in Chinese with English Abstract)

Huang, J. Y., Hu, S. X., Zhang, Q. Y., et al., 2019a. Gondolelloid Multielement Conodont Apparatus (*Nicoraella*) from the Middle Triassic of Yunnan Province, Southwestern China. *Palaeogeography*, *Palaeoclimatology*, *Palaeoecology*, 522: 98–110. https://doi.org/10.1016/j.palaeo.2018.07.015

Huang, J. Y., Martínez-Pérez, C., Hu, S. X., et al., 2019b. Middle Triassic Conodont Apparatus Architecture Revealed by Synchrotron X-Ray Microtomography. *Palaeoworld*, 28(4): 429–440. https://doi.org/10.1016/j.palwor.2018.08.003

Huang, J. Y., Martínez-Pérez, C., Hu, S. X., et al., 2019c. Apparatus Architecture of the Conodont Nicoraella Kockeli (Gondolelloidea, Prioniodinina) Constrains Functional Interpretations. *Palaeontology*, 62(5): 823–835. https://doi.org/10.1111/pala.12429

Janvier, P., 1995. Conodonts Join the Club. *Nature*, 374(6525): 761–762.

https://doi.org/10.1038/374761a0

Jiang, D. Y., Motani, R., Hao, W. C., et al., 2009. Biodiversity and Sequence of the Middle Triassic Panxian Marine Reptile Fauna, Guizhou Province, China. *Acta Geologica Sinica—English Edition*, 83(3): 451–459. https://doi.org/10.1111/j.1755-6724.2009.00047.x

Kolar-Jurkovšek, T., Martínez-Pérez, C., Jurkovšek, B., et al., 2018. New Clusters of Pseudofurnishius Murcianus from the Middle Triassic of Slovenia (Dinarides). *Bulletins of American Paleontology*, 395/396: 149–163. https://doi.org/10.32857/bap.2018.395.11

Kozur, H., 1989. The Taxonomy of the Gondolellid Conodont in the Permian and Triassic. *CFS Courier Forschungsinstitut Senckenberg*, 117: 409–469

Kozur, H., Mock, R., 1991. New Middle Carnian and Rhaetian Conodonts from Hungary and the Alps. Stratigraphic Importance and Tectonic Implications for the Buda Mountains and Adjacent Areas. *Jahrbuch der Geologischen Bundesanstalt*, 134(2): 271–297

Luo, M., Chen, Z. Q., Hu, S. X., et al., 2013. Carbonate Reticulated Ridge Structures from the Lower Middle Triassic of the Luoping Area, Yunnan, Southwestern China: Geobiologic Features and Implications for Exceptional Preservation of the Luoping Biota. *PALAIOS*, 28(8): 541–551. https://doi.org/10.2110/palo.2012.p12-122r

Luo, M., Chen, J. T., Qie, W. K., et al., 2021. Microbially Induced Carbonate Precipitation in a Middle Triassic Microbial Mat Deposit from Southwestern China: New Implications for the Formational Process of Micrite. *Journal of Earth Science*, 32(3): 633–645. https://doi.org/10.1007/s12583-020-1075-6

Luo, M., Gong, Y. M., Shi, G. R., et al., 2018. Palaeoecological Analysis of Trace Fossil Sinusichnus Sinuosus from the Middle Triassic Guanling Formationin Southwestern China. *Journal of Earth Science*, 29(4): 854–863. https://doi.org/10.1007/s12583-018-0794-4

Luo, M., Hu, S. X., Benton, M. J., et al., 2017. Taphonomy and Palaeobiology of Early Middle Triassic Coprolites from the Luoping Biota, Southwest China: Implications for Reconstruction of Fossil Food Webs. *Palaeogeography, Palaeoclimatology, Palaeoecology*, 474: 232–246. https://doi.org/10.1016/j.palaeo.2016.06.001

Luo, M., Shi, G. R., Hu, S. X., et al., 2019. Early Middle Triassic Trace Fossils from the Luoping Biota, Southwestern China: Evidence of Recovery from Mass Extinction. *Palaeogeography, Palaeoclimatology, Palaeoecology*, 515: 6–22. https://doi.org/10.1016/j.palaeo.2017.11.028

Ma, Z. X., Hu, S. X., Liu, X. T., et al., 2021. The Link between Exceptional Fossil Preservation and Palaeo-Redox Conditions in the Middle Triassic Luoping Biota from South China. *Geological Journal*, 56(12): 6231–6244. https://doi.org/10.1002/gj.4106

Mastandrea, A., Ietto, F., Neri, C., et al., 1997. Conodont Biostratigraphy of the Late Triassic Sequence of Monte Cocuzzo (Catena Costiera, Calabria, Italy). *Rivista Italiana di Paleontologia e Stratigrafia*, 103(2): 173–182. https://doi.org/10.13130/2039-4942/5288

Mastandrea, A., Neri, C., Ietto, F., et al., 1999. *Misikella ultima* Kozur & Mock, 1991: First Evidence of Late Rhaetian Conodonts in Calabria (Southern Italy). *Bollettino della Societa Paleontologica Italiana*, 37(2/3): 497–506

Mellgren, J. S., Eriksson, M. E., 2006. A Model of Reconstruction for the Oral Apparatus of the Ordovician Conodont Genus *Protopanderodus* Lindström, 1971. *Transactions of the Royal Society of Edinburgh*: *Earth Sciences*, 97(2): 97–112. https://doi.org/10.1017/s0263593300001425

Orchard, M. J., Rieber, H., 1999. Multielement *Neogondolella* (Conodonta, Upper Permian–Middle Triassic). *Bollettino della Societa Paleontologica Italiana*, 37(2/3): 475–488

Purnell, M. A., 1994. Skeletal Ontogeny and Feeding Mechanisms in Conodonts. *Lethaia*, 27(2): 129–138. https://doi.org/10.1111/j.1502-3931.1994.tb01567.x

Purnell, M. A., Aldridge, R. J., Donoghue, P. C. J., et al., 1995. Conodonts and the First Vertebrates. *Endeavour*, 19(1): 20–27. https://doi.org/10.1016/0160-9327(95)98890-r

Purnell, M. A., Donoghue, P. C. J., 1997. Architecture and Functional Morphology of the Skeletal Apparatus of Ozarkodinid Conodonts. *Philosophical Transactions of the Royal Society of London Series B*: *Biological Sciences*, 352(1): 1545–1564. https://doi.org/10.1098/rstb.1997.0141

Purnell, M. A., Donoghue, P. C. J., 1998. Skeletal Architecture, Homologies and Taphonomy of Ozarkodinid Conodonts. *Palaeontology*, 41(1): 57–102

Purnell, M. A., Donoghue, P. C. J., Aldridge, R. J., 2000. Orientation and Anatomical Notation in Conodonts. *Journal of Paleontology*, 74(1): 113–122

Ramovš, A., 1977. The Reconstructed Skeletal Apparatus of *Pseudofurnishius murcianus* (Conodontophorida) in the Middle Triassic of Slovenia (NW Jugoslavia). *Neues Jahrbuch für Geologie und Paläontologie*: *Abhandlungen*, 153(3): 361–399

Ramovš, A., 1978. Mitteltriassische Conodonten-Clusters in Slowenien, NW Jugoslawien. *Paläontologische Zeitschrift*, 52(1): 129–137. https://doi.org/10.1007/bf03006734

Rieber, H., 1980. Ein Conodonten-Cluster aus der Grenzbitumenzone (Mittlere Trias) des Monte San Giorgio (Kt. Tessin /Schweiz). *Annalen des Naturhistorischen Museums in Wien*, 83: 265–274

Roghi, G., Mietto, P., Vecchia, F. M. D., 1995. Contribution to the Conodont Biostratigraphy of the Dolomia di Forni (Upper Triassic, Carnia, NE Italy). *Memorie Scienze Geologiche*, 47: 125–133

Schmidt, H., 1934. Conodonten-Funde in Ursprünglichem Zusammenhang. *Palaeontologische Zeitschrift*, 16(1): 76–85. https://doi.org/10.1007/bf03041668

Scott, H. W., 1934. The Zoological Relationships of the Conodonts. *Journal of Paleontology*, 8(4): 448–455

Sun, Z. Y., Hao, W. C., Sun, Y. L., et al., 2009. The Conodont Genus Nicoraella and a New Species from the Anisian of Guizhou, South China. *Neues Jahrbuch für Geologie und Paläontologie-Abhandlungen*, 252(2): 227–235. https://doi.org/10.1127/0077-7749/2009/0252-0227

Sun, Z. Y., Liu, S., Ji, C., et al., 2021. Gondolelloid Multielement Conodont Apparatus (*Scythogondolella*) from the Lower Triassic of Jiangsu, East China, Revealed by High-Resolution X-Ray Microtomography. *Palaeoworld*, 30(2): 286–295. https://doi.org/10.1016/j.palwor.2020.06.001

Sun, Z. Y., Liu, S., Ji, C., et al., 2020. Synchrotron-Aided Reconstruction of the Prioniodinin Multielement Conodont Apparatus (*Hadrodontina*) from the Lower Triassic of China. *Palaeogeography, Palaeoclimatology, Palaeoecology*, 560: 109913. https://doi.org/10.1016/j.palaeo.2020.109913

Suttner, T. J., Kido, E., Briguglio, A., 2018. A New Icriodontid Conodont Cluster with Specific Mesowear Supports an Alternative Apparatus Motion Model for Icriodontidae. *Journal of Systematic Palaeontology*, 16(11): 909–926. https://doi.org/10.1080/14772019.2017.1354090

Sweet, W. C., Bergström, S. M., 1969. The Generic Concept in Conodont Taxonomy. *Proceedings North American Paleontological Convention*, 1: 29–42

Sweet, W. C., Donoghue, P. C. J., 2001. Conodonts: Past, Present, Future. *Journal of Paleontology*, 75(6): 1174–1184. https://doi.org/10.1017/

s0022336000017224

Takahashi, S., Yamakita, S., Suzuki, N., 2019. Natural Assemblages of the Conodont *Clarkina* in Lowermost Triassic Deep-Sea Black Claystone from Northeastern Japan, with Probable Soft-Tissue Impressions. *Palaeogeography, Palaeoclimatology, Palaeoecology*, 524: 212–229. https://doi.org/10.1016/j.palaeo.2019.03.034

von Bitter, P. H., 1976. The Apparatus of *Gondolella sublanceolata* Gunnell, Conodontophorida, Upper Pennsylvanian, and Its Relationship to *Illinella typica* Rhodes. *Life Science Contributions of the Royal Ontrio Museum*, 109: 1–44

von Bitter, P. H., Merrill, G. K., 1998. Apparatus Composition and Structure of the Pennsylvanian Conodont Genus *Gondolella* Based on Assemblages from the Desmoinesian of Northwestern Illinois, U.S.A. *Journal of Paleontology*, 72(1): 112–132. https://doi.org/10.1017/s0022336000024057

von Bitter, P. H., Purnell, M. A., Tetreault, D. K., et al., 2007. Eramosa Lagerstätte—Exceptionally Preserved Soft-Bodied Biotas with Shallow-Marine Shelly and Bioturbating Organisms (Silurian, Ontario, Canada). *Geology*, 35(10): 879–882. https://doi.org/10.1130/g23894a.1

Wardlaw, B. R., Nestell, M. K., 2010. Three Jinogondolella Apparatuses from a Single Bed of the Bell Canyon Formation in the Apache Mountains, West Texas. *Micropaleontology*, 56(1/2): 195–212. https://doi.org/10.47894/mpal.56.1.07

Wen, W., Zhang, Q. Y., Hu, S. X., et al., 2013. Coelacanths from the Middle Triassic Luoping Biota, Yunnan, South China, with the Earliest Evidence of Ovoviviparity. *Acta Palaeontologica Polonica*, 58(1): 175–193. https://doi.org/10.4202/app.2011.0066

Wen, W., Zhang, Q. Y., Hu, S. X., et al., 2012. A New Genus of Basal Actinopterygian Fish from the Anisian (Middle Triassic) of Luoping, Yunnan Province, Southwest China. *Acta Palaeontologica Polonica*, 57(1): 149–160. https://doi.org/10.4202/app.2010.0089

Yan, C. B., Jiang, H. S., Lai, X. L., et al., 2015. The Relationship between the "Green-Bean Rock" Layers and Conodont *Chiosella timorensis* and Implications on Defining the Early-Middle Triassic Boundary in the Nanpanjiang Basin, South China. *Journal of Earth Science*, 26(2): 236–245. https://doi.org/10.1007/s12583-015-0535-x

Zeng, W. P., Purnell, M. A., Jiang, H. S., et al., 2021. Late Triassic (Norian) Conodont Apparatuses Revealed by Conodont Clusters from Yunnan Province, Southwestern China. *Journal of Earth Science*, 32(3): 709–724. https://doi.org/10.1007/s12583-021-1459-2

Zhang, M. H., Jiang, H. S., Purnell, M. A., et al., 2017. Testing Hypotheses of Element Loss and Instability in the Apparatus Composition of Complex Conodonts: Articulated Skeletons of Hindeodus. *Palaeontology*, 60(4): 595–608. https://doi.org/10.1111/pala.12305

Zhang, Q. Y., Zhou, C. Y., Lu, T., et al., 2009. A Conodont-Based Middle Triassic Age Assignment for the Luoping Biota of Yunnan, China. *Science in China Series D: Earth Sciences*, 52(10): 1673–1678. https://doi.org/10.1007/s11430-009-0114-z

Zhang, S. X., 1998. A Review on Apparatus Reconstruction of Conodonts Taking Triassic Elements as an Example. *Acta Micropalaeontologica Sinica*, 15(2): 111–124 (in Chinese with English Abstract)